Journal of the Arkansas Academy of Science

Volume 49 Article 32

1995

Spectroscopic Temperature Measurements for a Direct Current Arcjet Diamond Chemical Vapor Deposition Reactor

Scott W. Reeve
Naval Air Warfare Center

Wayne A. Weimer
Naval Air Warfare Center

Spectroscopic Temperature Measurements for a Direct Current Arcjet Diamond Chemical Vapor Deposition Reactor

Scott W. Reeve and Wayne A. Weimer
Chemistry Division, Research Department
Naval Air Warfare Center
China Lake, CA 93555

Abstract

The diamond thin film commercial market is projected to exceed one billion dollars by the year 2000. Potential applications of diamond thin films range from cutting tools to electronics to medical devices. The explosion of interest in this field results from the extreme properties diamond possesses: it is the hardest material known to man and yet, has a coefficient of friction similar to Teflon; its ability to conduct heat is five times that of copper; and diamond is completely inert. However, despite the tremendous economic incentive, there are still several technological barriers preventing diamond film scale-up to commercial production. Included among these are a fundamental understanding of the gas phase chemistry leading to diamond film formation and the lack of a reliable *in situ*, on-line Chemical Vapor Deposition (CVD) monitoring capability. Here we describe the use of optical emission spectroscopy (OES) as a possible direct current CVD plasma jet on-line monitor. Specifically, OES spectra from the C_2 radical, an intermediate species in the diamond CVD process, is utilized to obtain plasma gas temperatures *in situ*. Additionally, the reliability of a plasma gas temperature determined from OES is examined with Laser-Induced-Fluorescence (LIF).

Introduction

The material properties of diamond can be described by superlatives. Diamond is the hardest material known to man and possesses the highest thermal conductivity. It's coefficient of friction is similar to that of Teflon and, with the exception of a small window from 3-5 μm, diamond is transparent across the entire optical spectrum (Celii and Butler, 1991). Due to these extreme properties diamond is the material of choice for a remarkably diverse range of potential commercial applications. Examples include heat transfer substrates for computer chips as well as coatings for machine parts and cutting tools (Bigelow, 1993, Sussmann, 1993). *Conservative* projections predict the commercial market for diamond thin films will surpass $1,000,000,000 by the year 2000 (Bigelow, 1993). Currently, the cost of a 2.54 cm x 2.54 cm x 1 mm diamond film is -$10,000. To become economically feasible, this cost will need to be lowered by at least two orders of magnitude (Craig, 1992). Thus, the film growing process will need to be optimized before the full potential of diamond thin films can be realized.

Diamond thin films and coatings have been grown by several different chemical vapor deposition (CVD) techniques including hot filament CVD (Godbole and Narayan, 1992), microwave plasma CVD (Zhu et al., 1990), oxyacetylene torch CVD (Snail and Hanssen, 1991), and direct current (DC) plasma jet CVD (Reeve et al., 1993). In each case, a small amount of methane (or some other hydrocarbon) is injected into a hydrogen flow with the chemical reactions being initiated by the hot filament or the plasma (Butler and Woodin, 1993). Presumably, after a series of hydrogen abstractions the reactive carbon species encounters the growth surface and becomes incorporated into the diamond film although the chemical sequence for the conversion of methane gas into diamond in CVD reactors and the gas phase diamond growth precursors are still subjects of considerable debate.

While each of the methods listed above produces nearly identical polycrystalline films, the rate of film deposition is highly dependent upon the technique used. To date, the highest linear deposition rates have been obtained with the DC plasma jet (Ohtake and Yoshikawa, 1990). Because this represents the greatest potential for production scale-up, we focussed our attention on this CVD reactor. In this report, we present Optical Emission Spectrosscopy (OES) and Laser-Induced-Fluorescence (LIF) spectra for the C_2 species observed under typical diamond growth conditions in the DC plasma jet apparatus at China Lake, California. One of the objectives of the OES experiments was to determine if information beyond the obvious plasma parameters, such as emitting species identification and the corresponding excited state population distributions, could be obtained from the spectra. Therefore, a key feature of the OES work is the development of a method to extract plasma gas temperatures from the spatially resolved spectroscopic measurements. A comparison of the gas temperature obtained from the OES spectra with preliminary LIF measurements suggests

OES may be a useful diamond deposition process temperature monitor. Parenthetically, the quality and deposition rate of diamond thin films are highly dependent upon the temperature of the plasma gas during film growth (Celii and Butler, 1991). Thus, the plasma gas temperature is a critical parameter to monitor. In addition, the plasma gas temperature profile is needed as input for chemical kinetic models such as the CHEMKIN/PREMIX code (Reeve et al., 1993). It was predictions from a CHEMKIN calculation, that led us to an optimization strategy that, simultaneously, doubled the mass deposition rate and increased the quality of the films grown (Reeve and Weiner, 1994).

A diagram of the China Lake DC plasma jet CVD reactor together with a schematic of the OES and LIF apparatus is shown in Fig. 1. Diamond thin films are grown by injecting a mixture of hydrogen and methane gas, downstream of the electrode gap, into a flowing argon plasma operated at ~60 Torr reactor pressure. Note, argon is the **only** gas to pass through the electrode gap. The reactive high velocity plasma (~6000m/s) then impinges at normal incidence onto a molybdenum substrate. The substrate is mounted on a water cooled copper block so that a temperature of 1000°C can be maintained at the growth surface. Nominal operating conditions are given in Table 1. The China Lake DC plasma jet CVD reactor has previously demonstrated the ability to produce high quality diamond films as evaluated by both Raman spectroscopy and optical microscopy (Reeve et al., 1993).

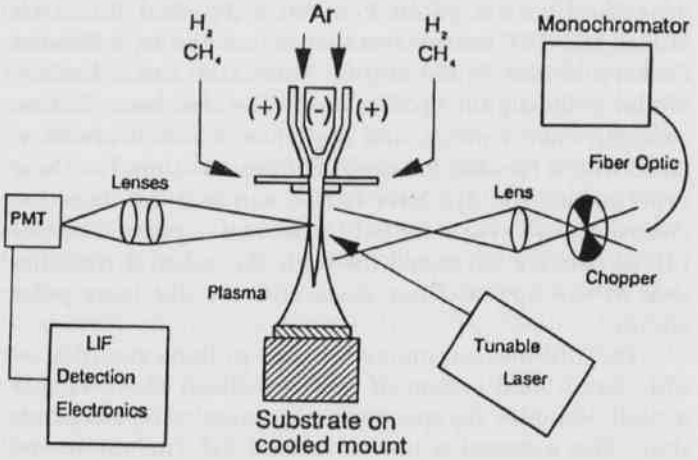

Fig. 1. Schematic of the China Lake DC plasma jet diamond CVD reactor along with the Optical Emission Spectroscopy and Laser-Induced-Fluorescence diagnostic capabilities.

Table 1. Operating Parameters for the China Lake DC Plasma Jet CVD Reactor.

DC voltage	20V
DC Current	140-150A
Reactor Pressure	55-60 Torr
Substrate Material	Molybdenum (25mm x 38mm)
Plasma Gun-Substrate Distance	~2.5 cm (~ 1 inch)
Gas Flow Rates	
Ar	13.7 slm
H_2	5.4 slm
CH_4	150-700 sccm

Results and Discussion

Optical Emission Spectroscopy.--The OES experiment is quite simple and consists of imaging the illuminous plasma, with a 150mm focal length biconvex lens, onto the end of a 1.0 mm fiber optic bundle. The dispersed spectra were recorded with a Spex Model 1702 scanning monochromator (0.5nm bandpass) and a Hamamatsu Model R928 photomultiplier tube. To increase sensitivity, the emission spectra was chopped and the output from the photomultiplier was sent to a PAR Model 5208 lock-in amplifier. The spectral response of the spectrometer was calibrated with an Optronics Laboratories Model 220M tungsten lamp. To obtain spatially resolved OES spectra, the end of the fiber optic was translated within the image of the plasma.

The details of the nonlinear curve fitting procedure, developed to extract the plasma gas temperature from the OES spectra, are described in the April Journal of Vacuum Science and Technology A (Reeve and Weimer, 1995) and will not be reproduced here. A representative OES spectrum for the $d^3\Pi_g \rightarrow a^3\Pi_u$ ($\Delta v=0$) Swan band emission of the C_2 radical is shown in Fig. 2 along with the results obtained from this curve fitting procedure. The spectrum in Fig. 2 was taken at an axial position of 2.36 cm above the growth surface. The vibrational and rotational temperatures, at this position, are 4646 K and 3301 K, respectively. While the agreement between the observed data points and the fitted spectrum is quite good, the validity of using an excited state *effective* rotational temperature to estimate the plasma gas temperature warrants some discussion. For a temperature determined from an emission spectrum to have meaning, the species responsible for the radiation must be thermalized. The quality of the curve fit to the data in Fig. 2 suggests the C_2 rotational and vibrational levels in the $d^3\Pi_g$ electronic state can be described by a Boltzmann distribution. While a system in thermodynamic equilibrium will have Boltzmann distributions for the gas, electronic,

vibrational, and rotational energies that can be defined by a single temperature, in reacting plasmas, departures from thermodynamic equilibrium are common for excited species (Hertzberg, 1950). Thus, Boltzmann distributions defined by different temperatures can be expected (Reeve and Weimer, 1995). In Fig. 2, the observed temperature difference is believed to be a direct consequence of an electron impact excitation mechanism for the C_2 species in the DC plasma jet.

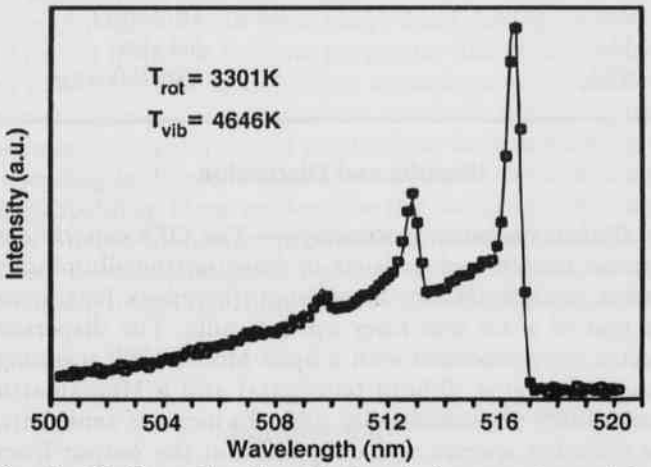

Fig. 2. C_2 Swan band optical emission spectrum taken 2.36 cm above the substrate during diamond thin film growth.

Optical emission can be produced by three different processes: chemiluminescent reaction, thermal excitation, and electron impact (Raiche and Jefferies, 1993). Each mechanism will produce qualitatively different emission spectra. For example, a thermal excitation mechanism will produce an excited state species with $T_{gas}=T_{vibrational}=T_{rotational}$. Based on the observed differences in $T_{vibrational}$ and $T_{rotational}$, this possibility can be excluded. Although we cannot rule out a chemiluminescent reaction as being the dominant excitation process for the C_2 species in our system, there is evidence to suggest the C_2 emission is the result of an electron impact mechanism.

An electron impact excitation mechanism would produce an excited electronic state vibrational distribution that is governed by the Franck-Condon overlap between the upper and lower electronic states (Raiche and Jefferies, 1993). In addition, because the mass of an electron is small relative to the mass of the C_2 molecule, no appreciable change from the lower state rotational energy distribution would be expected for the upper electronic state (Hertzberg, 1950). Given a thermalized temperature for the lower electronic state ($a^3\Pi_u$) of C_2, we can impose the Franck-Condon transition probabilities, predict the excited electronic state population distributions, and calculate the resulting vibrational and rotational temperatures in the $d^3\Pi_g$ assuming a Boltzmann distribution (Hertzberg, 1950). Thus, and electron colliding with and electronically exciting a C_2 molecule, in the $a^3\Pi_u$ electronic state and initially thermalized at T_{gas}=3301 K, would produce a vibrational distribution defined by $T_{vibrational}$=4710K and a rotational distribution defined by $T_{rotational}$=3301 K in the upper $d^3\Pi_g$ state. A comparison with the OES temperatures in Fig. 2 is unmistakable and suggests the C_2 emission here is the result of an electron impact excitation mechanism. Moreover, the Franck-Condo analysis indicates the rotational temperature of $d^3\Pi_g$ should provide some measure of the plasma gas temperature.

Laser Induced Fluorescence.--The LIF experiment utilized a Lumonics Model 860-4 exciter laser to pump a Lumonics Model EPD-330 dye laser capable of producing narrow band (0.003 nm) pulsed (~17 ns pulses) tunable radiation with an energy of ~12 mJ/pulse. Due to the reactor geometry, a relatively long focal length lens (300 mm) was used to focus the beam into the plasma jet. The diameter of the beam in this configuration is approximately 80 μm, still small relative to the spatial dimensions of the system. The transient LIF signals were collected at a right angle to the excitation beam and detected with an RCA Model 1P28 photomultiplier tube positioned behind an aperture to block scattered laser light and a wavelength calibrated optical filter stack designed to pass radiation over a limited wavelength range (~20 nm) appropriate for C_2 detection. The photomultiplier signals are processed with a gated Princeton Applied Research Model 162/164 boxcar averager connected to a Hewlett Packard Model 3455A digital voltmeter and a LeCroy Model 9400 digital oscilloscope. The dye laser, boxcar averager, energy meter, and digital oscilloscope are interfaced with a Hewlett Packard 9836 workstation. For these experiments, the dye laser is free run and the detection electronics are synchronized to each laser pulse. The raw LIF signals are corrected for both the spectral transmission of the optical filter stack and the dye laser pulse energy.

The LIF measurements are also probing the $d^3\Pi_g \leftarrow a^3\Pi_u$ Swan band system of the C_2 radical. However, LIF actually samples C_2 species in the lower $a^3\Pi_u$ electronic state. This metastable state is located 716 cm^{-1} above and is thermally populated by the ground electronic state. As a result, the rotational and vibrational distributions in the $a^3\Pi_u$ should be thermalized with the plasma gas temperature. The spectral resolution for the LIF measurements are determined by the excitation laser which has a narrow linewidth of 0.003 nm. At this resolution, we are able to excite individual P(ΔJ = -1), Q(ΔJ = 0), and R(ΔJ =1) branch transitions from the $a^3\Pi_u$ electronic state to

the $d^3\Pi_g$ state. The v' - v" = 0 Swan bands near 516 nm are the strongest C_2 transitions in the visible and were chosen for the preliminary measurements. While we could have theoretically excited and detected the $d^3\Pi_g$ fluorescence at 516 nm, laser scatter from the reactor walls was a severe problem and facilitated the need to choose a detection wavelength well separated from the excitation wavelength to avoid saturation of the photomultiplier. Therefore, for the measurements reported here, we excite the $d^3\Pi_g \leftarrow a^3\Pi_u$ (0,0) transitions at 516 nm and collect the total fluorescence signal from the $d^3\Pi_g \rightarrow a^3\Pi_u$ (0,1) Swan band near 560 nm. With this detection scheme, we are able to observe 21% of the fluorescence.

Another factor which complicates the LIF detection is the plasma emission from the C_2 species. An illustration of this background emission in the observed fluorescence is provided by the time resolved signal in Fig. 3. The top trace was recorded with the plasma on and no CH_4 flow in the reactive gas mixture. Note the laser scatter from the reactor walls in the top trace. The scatter results from the asymtotic band cutoff of the optical filter stack. With a filter stack centered at 520 nm, this laser scatter simply swamps the fluorescence signal. The bottom trace in Fig. 3 was taken with the plasma on and a CH_4 flow typical for diamond growth conditions. The offset in the baseline is from the C_2 $d^3\Pi_g \rightarrow a^3\Pi_u$ Swan band emission at 560 nm. From the time resolved data, a C_2 $d_3\Pi_g$ state fluorescent lifetime can be obtained. The observed fluorescence decay is actually a convolution of the true molecular fluorescence with the response function of the instrument (Felker and Zewail, 1984). In this case, the top trace in Fig. 3 is a real time response to the 17 nanosecond laser pulse. Fitting the scattered intensity to an exponential function of time yields a time constant for the scattered signal decay of τ_{laser}=8.76 ns. With this value in hand, the convolution integral to extract the excited state lifetime can be evaluated. The resulting time resolved spectral fit assigns a fluorescent lifetime to the C_2 d state of 36.0 ns. Since this value is significantly shorter than the 120 ns collision free radiative lifetime, the time resolved spectra suggest the $d^3\Pi_g$ excited state is strongly quenched in the plasma jet, presumably through collisions with H_2 (Reeve and Weimer, 1995). Previously, we reported calculated values for the time duration between quenching collisions with hydrogen for the CH $A^2\Delta$ species (Reeve and Weimer, 1995). The measured C_2 d state lifetime is remarkably close to the $\tau_{quenching}$ value (33 ns) for the CH A state at 3000 K (Reeve and Weimer, 1995).

In addition to the time resolved fluorescence spectrum, we can measure the C_2 fluorescence intensity as a function of excitation wavelength. We do need to first correct the spectral intensity for the dye laser pulse energy and for the effects of the optical filter stack. A plot of the corrected intensity versus dye laser wavelength for the C2 d←a(0,0) Swan band is given in Fig. 4. Note, the spectra shown in Fig. 4 is qualitatively similar to the C_2 516 nm Swan band absorption spectrum (Bulewicz et al., 1970) and the C_2 516 nm Swam band spectrum obtained by degenerate four wave mixing (Nyholm et al., 1994) which have been reported previously. Both of these spectra were acquired in an oxyacetylene flame. Here, the assignment of the individual P and R branch transitions are facilitated by these previous studies together with computer simulations of the Δv=0 Swan band spectra. With the exception of the P branch bandhead region near 516.5 nm, the individual rotational transitions in Fig. 4 appear to be fully resolved. Keep in mind however, the C_2 Swan bands are $^3\Pi$-$^3\Pi$ electronic transitions and will consist of three sub-bands (Hertzberg, 1950). Thus, each rotational transition is actually a triplet whose splitting becomes larger with decreasing rotational quantum number J (Hertzberg, 1950). This splitting is not resolved for the P branch lines in Fig. 4, although the weaker R branch transitions, beginning at and extending to lower wavelengths, are fully resolved in some instances. Modification of the OES curve fitting routine to handle the high resolution LIF spectra is still in progress. Nevertheless, a rotational temperature can be estimated from Fig. 4 (following Bulewicz et al., 1970) by plotting the logarithm of the rotational population for the $a^3\Pi$ v=0 state, $\ln(N_J)$, versus the rotational energy (Hertzberg, 1950). The integrated signal intensity for each rotational line is converted to a population by dividing by the rotational degeneracy (Raiche and Jefferies, 1993). For a perfect Boltzmann distribution, a straight line graph with slope $-1/kT_{rotational}$ is expected. Figure 5 is a plot of Ln(intensity)/(2J + 1) versus the rotational energy taken from the date in Fig. 4. The linearity in Fig. 5 is an indication of the extent to which the C_2 $a^3\Pi_u$ state population is thermalized with the plasma gas temperature. The rotational temperature determined from the slope of the line in Fig. 5 is 3174 ± 388 K. The corresponding OES rotational temperature at this spatial position is 3301 K.

In summary, while a chemiluminescence excitation cannot be ruled out, the evidence suggests the C_2 emission in the DC plasma jet is the result of an electron impact excitation mechanism. As a result, the rotational temperature, determined from the OES spectra, should provide a non-intrusive monitoring capability for the diamond DC plasma jet CVD process. Gas temperatures and fluorescent lifetimes determined from the preliminary LIF measurements supply additional experimental evidence to support this conclusion. One does need to keep in mind however, several factors can influence the accuracy of the OES temperature determination including plasma instability, line-of-sight temperature variations,

changes in the plasma opacity, as well as drift in the sensitivity of the spectrometer. For the OES measurements reported here, we estimate the uncertainty to be ± 300 K.

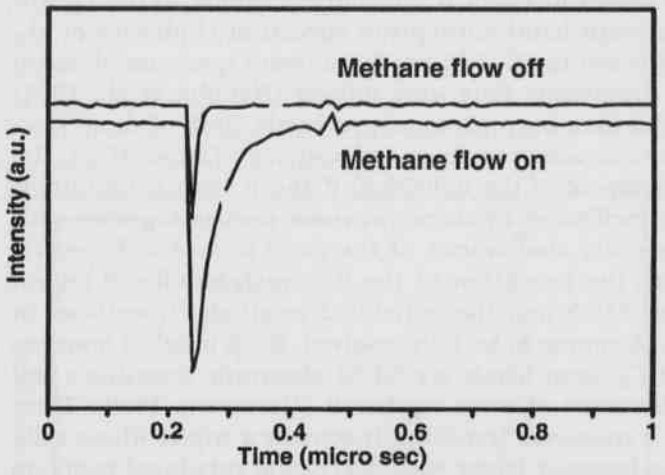

Fig. 3. Time resolved C_2 fluorescence signal recorded with the CH_4 flow on (lower trace) and off (upper trace).

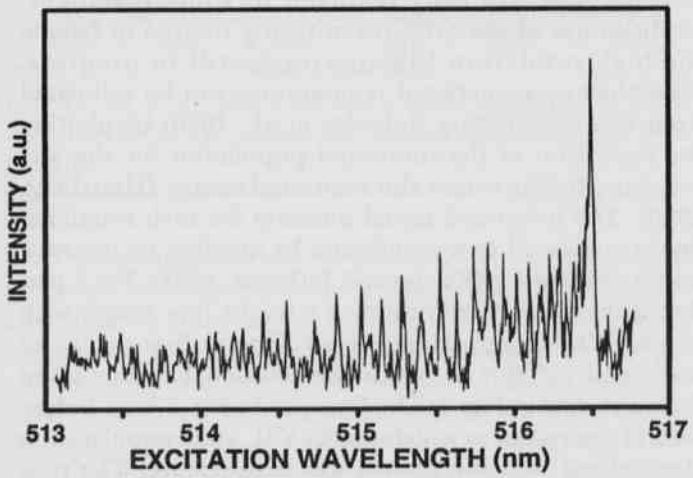

Fig. 4. Measured C_2 Laser-Induced-Fluorescence spectrum near bandhead in the C_2 Swan (0,0) band.

ACKNOWLEDGMENTS.--This work was supported by the Office of Naval Research. The authors wish to thank Drs. D.C. Harris, C.E. Johnson and D.S. Dandy for useful technical discussions. S.W. Reeve acknowledges the American Society for Engineering Education and the Office of Naval Research for a postdoctoral fellowship.

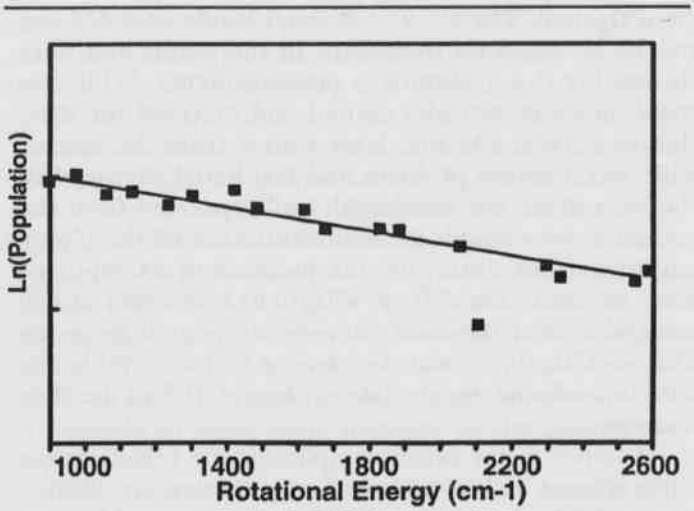

Fig. 5. Logarithmic plot of the rotational population versus the rotational energy for the a^3II_u electronic state.

Literature Cited

Bigelow, K. 1993. Progress in the commercialization of CVD diamond. Proc. 2nd Intl. Conf. Appl. Diamond Films and Related Materials. 5-12.

Bulewicz, E.M., P.J. Padley and **S.E. Smith.** 1970. Spectroscopic studies of C2, CH and OH radicals in low pressure acetylene + oxygen flames. Proc. Roy. Soc. A315:129-148.

Butler, J.E. and **R.L. Woodin.** 1993. Thin film diamond growth mechanisms. Phil. Trans. R. Soc. Lond. A342:209-224.

Celii, F.G. and **J.E. Butler.** 1991. Diamond chemical vapor deposition. Am. Rev. Phys. Chem. 42:643-684.

Craig, P. 1992. Thin-film-diamond derby. Cutting Tool Engineering. February 1992, 44.

Felker, P.M. and **A.H. Zewail.** 1984. Dynamics of Intramolecular Vibrational Energy Redistribution(IVR) II. Excess Energy Dependence. J. Chem. Phys. 1984. 82:2975-2993.

Godbole, V.P. and **J. Narayan.** 1992. Nucleation and growth of diamond on $FeSi_2$/Si substrates by hot filament chemical vapor deposition. J. Appl. Phys. 71:4944-4948.

Herzberg. G. 1950. Molecular Spectra and Molecular Structure: I. Spectra of Diatomic Molecules, 2nd edition. D. Van Nostrand Company, Inc.

Nyholm, K., M. Kaivola and **C.O. Aminoff.** 1994. Detection of C_2 and temperature measurement in a flame using degenerate four wave mixing in a forward geometry. Optics Comm. 107:406- 410.

Ohtake, N. and **M. Yoshikawa.** 1990. Diamond film preparation by are discharge plasma jet chemical

vapor deposition in the methane atmosphere. J. Electrochem. Soc. 137:717-722.

Raiche, G. and **J.B. Jefferies.** 1993. Laser-induced fluorescence temperature measurements in a dc arcjet used for diamond deposition. Applied Optics. 32:4629-4635.

Reeve, S.W., W.A. Weimer and **F.M. Cerio.** 1993. Gas phase chemistry in a direct current plasma jet diamond reactor. J. Appl. Phys. 74:7521-7530.

Reeve, S.W. and **W.A. Weimer.** 1994. Optimizing the gas phase chemistry in a d.c. arcjet diamond chemical vapor deposition reactor. Thin Solid Films 253:103-108.

Reeve, S.W. and **W.A. Weimer.** 1995. Plasma diagnostics of a direct current arcjet diamond reactor. Part II: Optical emission spectroscopy. J. Vac. Sci. Technol. A. 13:359-367.

Snail, K.A. and **L.M. Hanssen.** 1991. High temperature, high rate homoepitaxial growth of diamond in an atmosphere pressure flame. J. Crystal Growth 112:651-659.

Sussmann, R.S. 1993. Diafilm. A new diamond material for optics and electronics. Industrial Diamond Review. February 1993:1-10.

Zhu, W., A.R. Inspektor, A.R. Badzian, T. McKenna and **R. Messier.** 1990. Effects of noble gases on diamond deposition from methane-hydrogen microwave plasmas. J. Appl. Phys. 68:1489-1496.